

Super-resolution processing for pulsed neutron imaging system using a high-speed camera

K. Ishizuka^{1#}, T. Kai², T. Shinohara², M. Segawa², K. Mochiki¹

¹*Tokyo City University, 1-28-1 Tamazutsumi, Setagaya-ku, Tokyo 158-8557, Japan*

²*Japan Atomic Energy Agency, 2-4 Shirakatashirane, Tokai-mura, Naka-gun, Ibaraki 319-1195, Japan*

a corresponding author: g1481002@tcu.ac.jp

Energy-selective neutron radiography using pulsed neutron sources and time-of-flight (TOF) spectroscopy have been recognized as a useful technique to observe texture of materials, atomic distribution and magnetic field. For this pulsed neutron imaging high-speed cameras were used to obtain time resolved transmission images and at the beam line NOBORU in the MLF of J-PARC the neutron resonance absorption imaging has been successfully demonstrated [1]. In the high-speed camera there is a trade-off between frame rate and pixel number. For the application of resonance absorption the speed is the highest priority. In the application the high-speed camera (Fastcam-SA1.1) was used at the speed of 125 kfps (8 μ s for one image) and the image size of 256 x 128 pixels was not enough for an ideal requirement. Furthermore MCPs which were the essential components for ultra-high sensitivity blurred images by the effect of divergence of electrons between MCPs.

To improve the blurred images and the insufficient pixel number we propose image

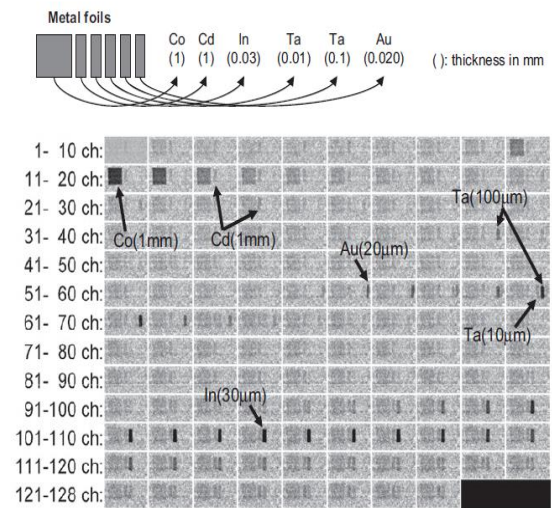
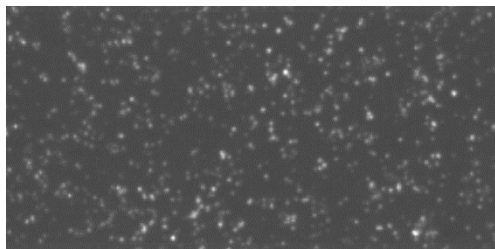


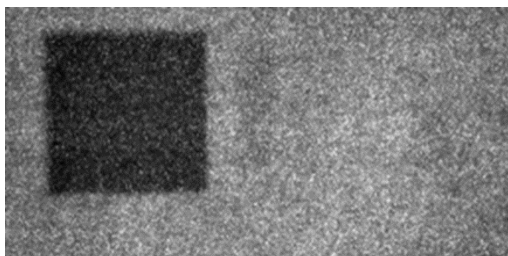
Fig.1 A set of neutron energy - dependent transmission images obtained by the high-speed camera. [1]

processing techniques of a center-of-gravity accumulation and super-resolution, respectively. The center-of-gravity accumulation method has been applied to resonance absorption images taken by the high-speed camera at NOBORU and shown in Fig.1. There are 128 images each of which was obtained by accumulation over the corresponding time-of-flight 2720 images. Figure 2 (a) shows one of the original images of the 11th channel. White spots were caused by neutron interactions in a fluorescent converter.

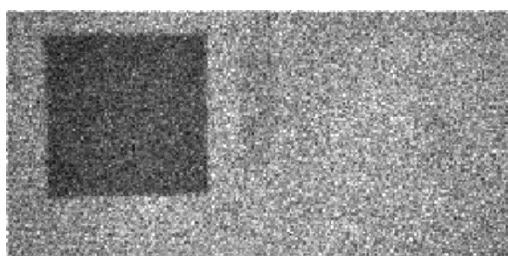
Each spots were blurred by the MCPs. Figure 2 (b) shows the accumulated image over 2720 data by ordinary method. Figure 2 (c) shows the accumulated image of center-of-gravity. The edge of the Co foil can be observed more clearly than that of the Fig.2 (b). Figure 2 (d) shows the accumulated image of center-of-gravity calculated to the second decimal place. The edge is still sharp and can be expected to be better if much data could be measured and processed. Figure 3 shows another example about the center-of gravity method. In the Fig.3 (b) the circles at the bottom part are clearly recognized than Fig.3 (a).



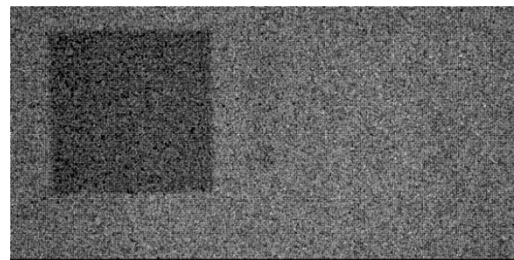
(a) Raw data from the high-speed camera.



(b) Ordinary cumulated image

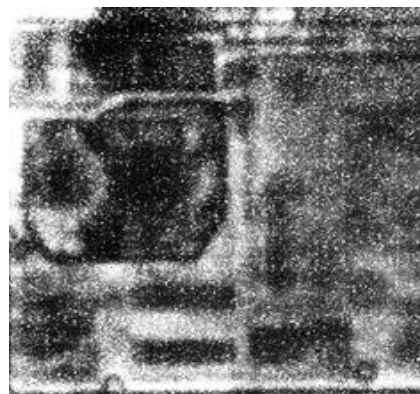


(c) Center-of-gravity method

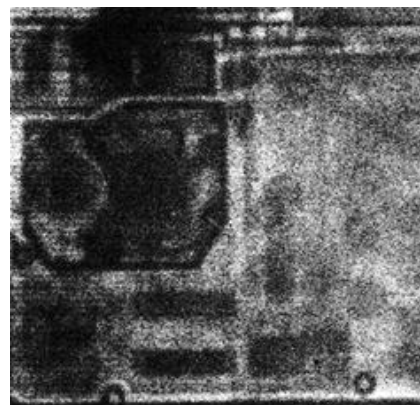


(d) Super-resolution method

Fig.2 Images concerning the 11th phase of the Fig.1. Images of (b), (c), and (d) are the results of accumulation over 2720 frames of corresponding 11th phase.



(a) Ordinary cumulated image



(b) Center-of-gravity method

Fig.3 Images of a digital camera.

Reference

- [1] T. Kai, et al., Nucl. Instr. And Meth. A **651** (2011) 126-130.